# Localization of Cell Surface Glycoproteins in Membrane Domains Associated with the Underlying Filament Network

E. ROOS,* H. SPIELE,* C. A. FELTKAMP,* H. HUISMAN,‡ F. A. C. WIEGANT,*
J. TRAAS,*, and D. A. M. MESLAND*
*Division of Cell Biology, The Netherlands Cancer Institute (Antoni van Leeuwenhoek Huis), 1066 CX
Amsterdam, The Netherlands, and ‡Central Laboratory of the Red Cross Blood Transfusion Service,
Amsterdam, The Netherlands. Dr. Wiegant's present address is Laboratory for Molecular Cell Biology,
University of Utrecht, The Netherlands. Dr. Traas's present address is Botanic Laboratory, Catholic
University of Nijmegen, The Netherlands. Dr. Mesland's present address is European Space Technology
and Research Center, Division TB, Noordwijk, The Netherlands.

ABSTRACT    To visualize the localization of cell surface constituents in relation to the plasma
membrane–associated filament network, we developed a method based on a combination of
immunogold labeling and dry-cleaving. For labeling we used trinitrophenyl-derivatized ligand,
anti-TNP antibodies, and protein A–coated colloidal gold. Dry-cleaving (Mesland, D. A. M.,
H. Spiele, and E. Roos, 1981, Exp. Cell Res., 132:169–184) involves cleavage of lightly fixed
critical point–dried cells by means of adhesive tape. Since cells cleave close to the cell surface,
the remaining layer is thin enough to be examined in transmission electron microscopy.

Using this method, we studied concanavalin A–binding constituents on the medium-facing
surface of H35 hepatoma cells. The distribution of the gold particles, which was partly
dispersed and partly patchy, coincided strikingly with membrane-associated filaments, and
label was virtually absent from areas overlying openings in the filament network. In stereo
pairs we observed the label to be localized to areas of somewhat enhanced electron density
at the plane of the membrane. These areas were interconnected in a pattern congruent with
the filament network.

Preliminary observations on wheat germ agglutinin receptors on the hepatoma cells as well
as concanavalin A receptors on isolated hepatocytes yielded comparable results. It thus
appears that surface glycoproteins, although seemingly randomly distributed as observed in
thin sections, may actually be localized to particular membrane domains associated with
underlying filaments.

Some cell surface proteins are relatively immobile (1–3) and
are not released by detergent extraction of cells (4–6), suggesting that they are firmly attached to the cytoskeleton.
Immobilization and detergent-resistant attachment of additional membrane proteins can be induced by interaction with
extracellular ligands (3, 7–11). Binding to such ligands may
result in transport of cell surface proteins to one side of the
cell (capping) and when this occurs co-capping of cytoskeletal
proteins is seen (12–16), again suggesting linkage between
membrane proteins and the cytoskeleton. Indeed, the existence of such linkages has been demonstrated electron microscopically (17). Several molecules putatively involved in this
linkage have been identified (18–21), as well as membrane

proteins that may bind directly to cytoskeletal components
(22–25), but their role is not yet entirely clear (26).

In contrast, many membrane proteins, including unbound
receptors, are mobile within the membrane (1, 2, 27). However, their diffusion rate is much lower than in artificial lipid
bilayers (28), indicating that lateral movement is constrained
by membrane-associated proteins. In erythrocytes, membrane-associated proteins are particularly well characterized,
and these cells are known to contain a submembranous actin–
spectrin network linked to integral membrane proteins (29,
30). When this network is detached, the lateral mobility of
membrane proteins strongly increases (31). The presence in
many cell types of fodrin, a protein closely related to spectrin,

and its submembranous localization (32–34), suggests that such a network is a general feature of cells, although its function is not necessarily comparable to that of the erythrocyte (35). Indeed, in membrane "blebs," which lack an associated cytoskeleton, the diffusion rate of surface proteins is much higher than in other parts of the cell (36). Apparently, the constraints are due to transient interactions with the cytoskeleton. It may then be assumed that such interactions keep even mobile proteins localized preferentially in areas where the network is attached to the membrane rather than homogeneously distributed. We present evidence supporting this notion in the case of concanavalin A (Con A)–binding proteins[1] of hepatoma cells.

This evidence was obtained with the use of dry-cleaving, a method developed by us to visualize submembranous structures in the electron microscope (3). Lightly fixed, critical point–dried cells on a grid covered with a carbon-over-Formvar film, are attached to adhesive tape and subsequently removed, which leads to cleavage of the cells close to the Formvar-attached membrane (see Fig. 1). The layer remaining on the grid is thin enough to be studied in a transmission electron microscope. The method was first applied to cells that had been cultured on the grids, exposing the substrate-facing membrane and associated network (37). Later we showed that also cells that had been fixed in suspension could be cleaved, after attachment to poly-L-lysine–coated, Formvar-covered grids (38). Thus, we demonstrated the presence of membrane-associated filament networks, of distinct morphology, in several different cell types (38).

We now show that also the medium-facing surface can be studied, after inversion of a fixed monolayer on a poly-L-lysine-coated grid (see Fig. 1). This allowed us to examine cells of which the medium-facing surface had been labeled immunocytochemically to visualize membrane-associated filaments and Con A–binding membrane proteins simultaneously. Thus, we observed that these membrane proteins were localized in areas overlying the network. Moreover, the label defined the plane of the membrane in stereo electron micrographs and highlighted within this plane areas of somewhat enhanced electron density to which all of the label was localized. These membrane areas were interconnected in a pattern congruent with the filament network. These observations suggested that plasma membranes contain protein-rich microdomains in areas associated with cytoskeletal filaments.

## MATERIALS AND METHODS

*Cell Preparation:* H35 hepatoma cells were cultured as previously described (38), except that they were grown in 16-mm multiwell plates on round plastic or glass coverslips. Preparation of cells was as described before (37–39). Briefly, cells were fixed in 0.1% glutaraldehyde, inverted on a grid (see below), treated with 1% tannic acid, postfixed with 0.5% OsO₄, stained with uranyl acetate, dehydrated, and critical point dried. Rat hepatocytes were isolated and cultured in Petriperm dishes as detailed previously (37), and treated as above. In all experiments, part of the cells were not critical point dried, but instead embedded in Epon using standard procedures.

*Inversion of the Monolayer:* After fixation in glutaraldehyde, part of the monolayer was cut free using the edge of an electron microscope grid, and detached by inserting the grid between the monolayer and the substrate. The detached cell layer was then inverted and positioned on a poly-L-lysine-coated, Formvar-carbon-covered grid, prepared as described previously (37), postfixed in OsO₄ and treated as described above.

*Dry-cleaving:* The grid with the dried cells was positioned, cell-side

[1] *Abbreviations used in this paper:* Con A, concanavalin A; TNP, trinitrophenyl.

down, on the sticky side of a clean piece of adhesive tape and gently pressed. Subsequently, the grid was removed, cleaving the cells and leaving the largest part of each cell on the tape. The grid was immediately viewed in the electron microscope, or stored for short periods in a dry environment. Further details are given in references 37–39. The whole procedure is illustrated in Fig. 1.

*Trinitrophenyl (TNP)–Con A:* 5 mg Con A and 100 mg α-methyl-mannoside (both from Sigma Chemical Co., St. Louis, MO) were dissolved in 4 ml phosphate-buffered saline (PBS). At room temperature, 3 mg trinitroben-zene–sulphonic acid in 1 ml of PBS was added dropwise under vigorous vortexing. The reaction was allowed to proceed for 30 min and then stopped by addition of 0.2 M glycine (40 ml). The mixture was concentrated under pressure in an Amicon filter unit (cut off: 10,000), diluted with PBS, concentrated again, and subsequently dialyzed for 48 h against three changes of 1 liter of PBS. The extinction of the resulting solution was measured at 280 nm and the Con A concentration adjusted to 1 mg/ml, using underivatized Con A as standard. Subsequently, the extinction at 338 nm was measured and the degree of substitution calculated based on a molecular extinction coefficient of 11,100 for TNP (40). The molar ratio of TNP and Con A was approximately 2, and could not be increased by prolonged incubation or with higher concentrations
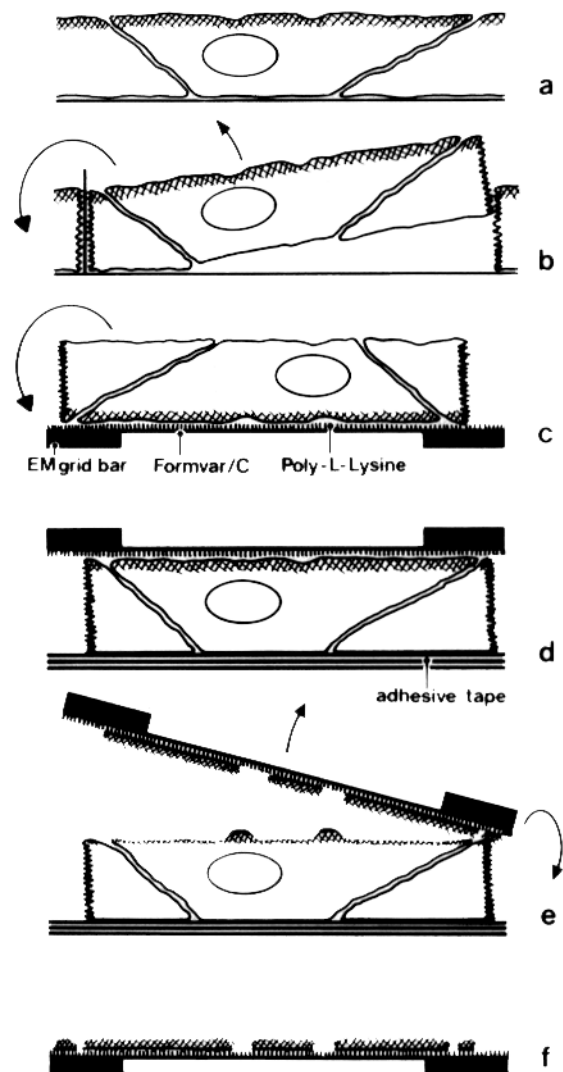


FIGURE 1   Schematic illustration of the dry-cleaving method as applied in this study. A piece of a glutaraldehyde-fixed monolayer of H35 hepatoma cells (a) is cut loose (b) and inverted onto a carbon-over-Formvar (Formvar/C) film-covered grid, coated with poly-L-lysine (c), treated with tannic acid and osmium tetroxide, dehydrated, and critical point dried. The grid is then placed cell-side down on adhesive tape (d), gently pressed, and removed (e), which leads to cleavage close to the grid (e). The resulting preparation (f) consists of the plasma membrane and a thin layer of cytoplasmic material.
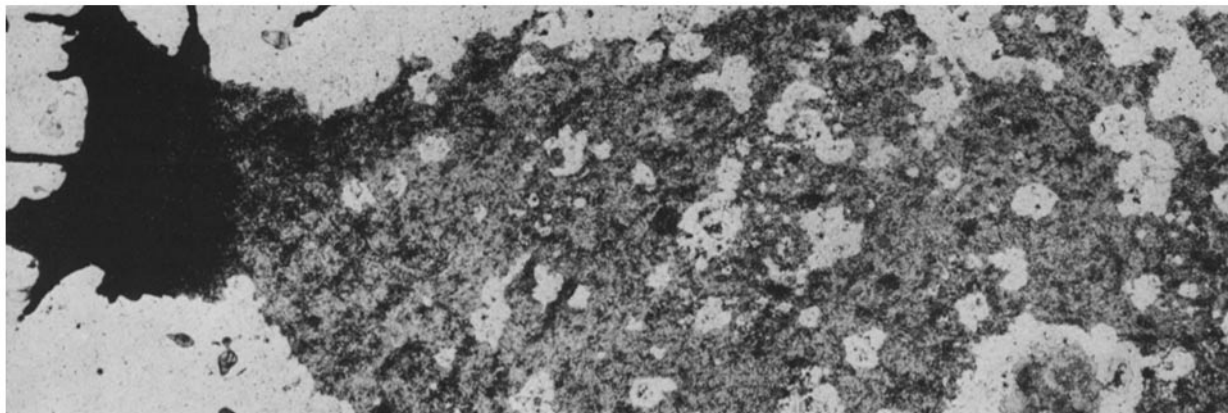
FIGURE 2   A low power micrograph of a preparation obtained by the dry cleaving method (see Fig. 1). The black area to the left is an uncleaved part of the cell. × 8,550.

of trinitrobenzene–sulphonic acid. Wheat germ agglutinin–TNP was prepared similarly, using N-acetylglucosamine (Sigma Chemical Co.) instead of α-methylmannoside. In this case the molar ratio was approximately 1.

*Anti-TNP Antibodies:*   TNP-derivatized bovine serum albumin (BSA) was prepared essentially as described above. Anti-TNP antibody was raised in a sheep by immunization with 1 mg TNP-derivatized BSA in complete Freund's adjuvant, followed after 4 wk by a second injection with 0.5 mg TNP-BSA in incomplete Freund's adjuvant. 1 wk later citrated plasma was obtained. The plasma was defibrinated and inactivated by heating for 1 h at 56°C.

*Protein A–Gold Conjugate:*   Protein A–coated gold particles with a diameter of 4–6 nm were prepared according to Slot and Geuze (41).

*Reaction with Lectins:*   Cells were usually prefixed with 0.1% glutaraldehyde in HMK buffer (0.1 M KCl, 3 mM MgCl₂, 10 mM HEPES, pH 6.9) for at least 15 min and then treated for at least 5 min with 20 mM glycine in PBS to quench unreacted aldehyde groups. Next, the cells were incubated at room temperature with 10–500 μg/ml Con A–TNP in PBS for 30 min. Controls were treated with Con A–TNP + 0.1 M α-methylmannoside or with PBS only. After three washes with PBS, anti-TNP antiserum was added in a 1:10 dilution, previously determined to be optimal. After 30 min, the cells were washed three times with 0.1% BSA in PBS, and then incubated with an optimal dilution of the protein A–gold suspension in 0.1% BSA in PBS, determined separately for each batch. Prior to use, this solution was centrifuged in a Beckman minifuge to remove aggregates. After three washes in PBS, with intervals of 10 min, and 1 wash in HMK buffer (37), the cells were postfixed in 0.1% glutaraldehyde in HMK buffer, and further treated as described under "cell preparation." Part of the dry-cleaved cells were embedded in Epon to be able to observe in thin sections whether the cell membrane and the label had remained intact during dry-cleaving. Furthermore, part of the cells were dried but not cleaved, and replicas of their upper surface were made as described previously (39), in order to observe the distribution of the label before attachment to the polylysine and before cleaving.

All incubations were usually performed at room temperature. In some cases cells were fixed with glutaraldehyde of 0°C and all procedures (inversion, labeling) up to and including fixation with OsO₄ were performed on ice in the cold room. In some experiments cells were incubated with Con A–TNP before fixation. After various periods at 37°C, cells were washed in several batches of PBS within 30 s, and fixed with 0.1% glutaraldehyde in HMK buffer.

*Electron Microscopy:*   Sections of embedded material (stained with lead acetate) and dry-cleaved preparations were observed in a Philips EM 301 electron microscope. Stereo micrographs were taken at tilt angles of +6° and −6°.

## RESULTS

### Dry-cleaving

Fig. 1 illustrates the dry-cleaving method as used in this study. The method was based on our observation that when a Formvar film–covered electron microscope grid with attached critical point–dried cells was placed, cell-side down, on the sticky side of adhesive tape (Fig. 1 d), lightly pressed, and subsequently removed (Fig. 1 e), the cells cleaved close to
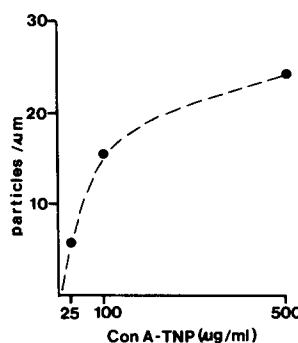


FIGURE 3   Number of gold particles per μm counted on thin sections of H35 hepatoma cells treated with various concentrations of Con A–TNP, followed by incubation with anti-TNP antibodies and protein A–gold. Shown are the results of a representative experiment.

the grid. Thus, the major part of each cell remained on the tape, and only the plasma membrane and a layer of associated cytoplasmic material remained on the grid (Fig. 1 f). This layer was thin enough to be examined in transmission electron microscopy.

In the present study we modified the method to visualize the medium-facing rather than the substrate-facing plasma membrane and associated material. A piece of a glutaraldehyde-fixed monolayer was cut out (Fig. 1 b), inverted, and placed on a poly-L-lysine-coated grid (Fig. 1 c) before further treatment and critical point drying. As a result, the medium-facing membrane was attached to the grid, and cells tended to cleave close to this membrane. Fig. 2 is a low power micrograph of such a preparation, showing both cleaved and uncleaved parts of a cell.

### Immunogold Labeling

Using this method we examined cells of which the medium-facing surface had first been labeled to localize particular cell surface constituents. We describe here the visualization of Con A–binding molecules on H35 hepatoma cells with the use of a novel cytochemical method, based on TNP–derivatized ligand, anti-TNP antibodies, and protein A–coated colloidal gold. Optimal conditions were first established using thin sections of embedded cells. Fig. 3 shows the number of particles per μm as a function of Con A–TNP concentration, using optimal concentrations of anti-TNP antiserum and protein A–gold. Fig. 4a shows a cell treated with 500 μg Con A–TNP per ml. Cells incubated with Con A–TNP in the presence of the hapten sugar α-methylmannoside (Fig. 4b), as well as cells incubated with PBS only before treatment with antiserum and protein A–gold, were virtually free of label.
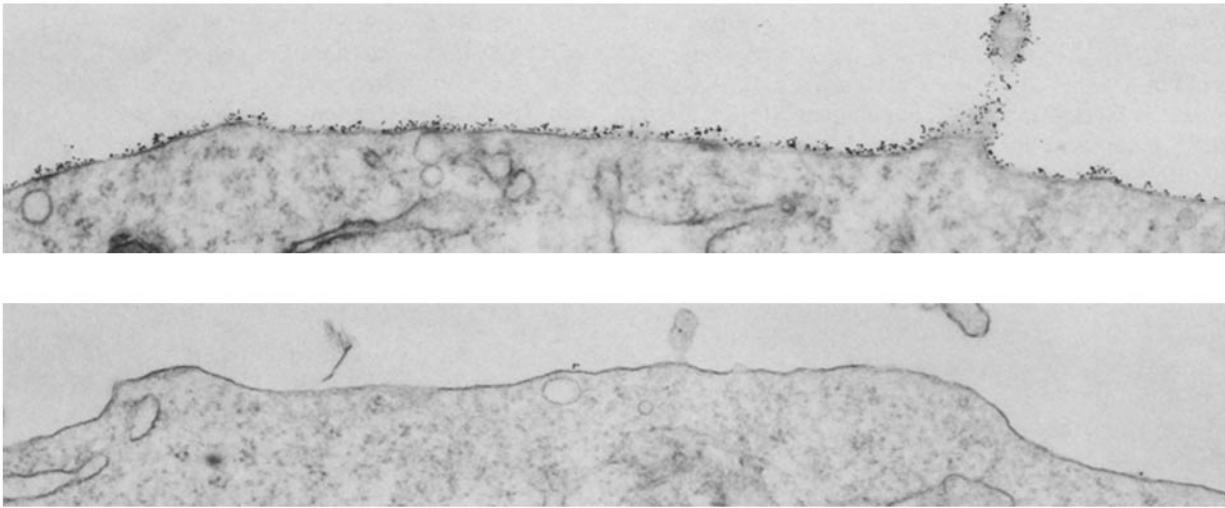
FIGURE 4   (Top) Part of a cell treated with 500 µg/ml Con A-TNP, followed by anti-TNP antibodies and protein A-gold. (Bottom) Same as a but treatment with Con A-TNP in the presence of 100 mM α-methylmannoside. × 47,500.
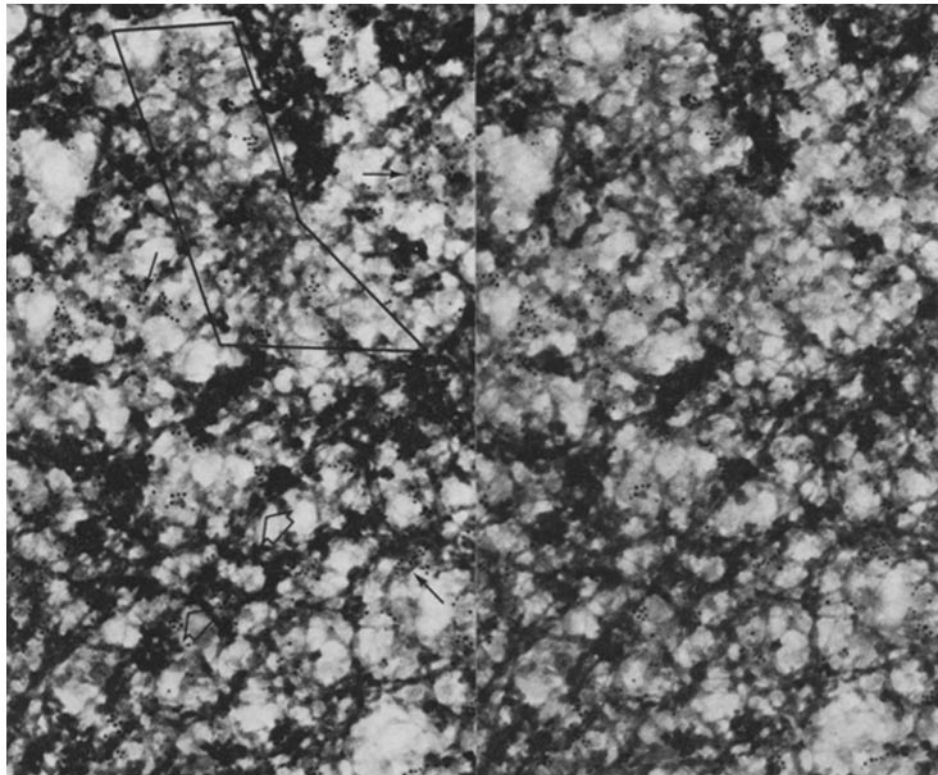


FIGURE 5   Stereo view of a dry-cleaved preparation of the medium-facing surface of a cell treated as in top panel of Fig. 4. The view is from inside the cell. The black areas constitute a dense network some distance from the membrane. Note long, straight filaments (open arrows). In some parts, e.g., the framed area, this layer appears to have been torn away. The gold particles are located at sites of enhanced electron density at the membrane (e.g., arrows). × 90,000.

## Immunogold-labeled, Dry-cleaved Preparations

Fig. 5 shows a stereo view of a dry-cleaved preparation of a labeled H35 hepatoma cell. The stereo pair is oriented such that the point of view is from within the cell through, first, the cortical filaments, second, the medium-facing membrane and, finally, the extracellularly located label. It can easily be seen that all of the label is located at approximately the same plane, which therefore should be a plane close to the extracellular face of the plasma membrane.

Closest to the viewer, i.e., at some distance intracellularly from the membrane, a dense array of knobby filaments with many associated proteins was seen to be present. These are the black areas in Fig. 5. Long, straight filaments were seen at this level (Fig. 5) as well as an occasional microtubule (not shown). The plane of cleavage was apparently within this layer and was irregular, so that in many areas this dense filament layer appeared to have been torn away (Fig. 5). Between this layer and the plasma membrane a network of various kinds of filaments was present, which could be most

easily seen in the areas where overlying filaments had been torn away. Figs. 6–8 show photographical enlargements of parts of Fig. 5. Short thin filaments (~2 nm) can be seen (Fig. 6), as well as short strands of ~6 nm diameter (Figs. 7 and 8) which in some areas appear to be arranged in a hexagonal pattern with a ~28-nm center-to-center distance (Fig. 8). This network appeared to terminate at a plane located at a small but distinct distance from the gold label.

## Distribution of the Label

As can be seen in Figs. 5–8, the gold label was partly dispersed and partly located in clusters of up to ~25 particles. The label was not randomly distributed but located preferentially where many filaments were present, and strikingly absent from membrane areas overlying openings in the network. Upon inspection of the stereo pairs, the label was found to be localized to areas of somewhat higher electron density. This was particularly evident in case of clustered particles. Filaments of the cortical network often terminated at or near such electron-dense areas (Fig. 6). The areas were interconnected and thus appeared to form a network of membrane domains.

The electron-dense membrane areas were also seen in dry-cleaved cells that had not been treated with Con A–TNP although less readily because these were not highlighted by the presence of label (Fig. 9). The empty membrane areas were not simply holes in the membrane, since such holes could be readily distinguished (Fig. 9). Furthermore, holes were not usually seen in thin sections of embedded, dry-cleaved cells (Fig. 10). The distribution of label was not different from that seen on non-cleaved cells. On replicas of the upper surface of dried but not cleaved cells (Fig. 11) label

was seen in particular areas in a pattern similar to that observed in dry-cleaved cells. In cells fixed in ice-cold glutaraldehyde, and treated at 0°C up to and including osmium tetroxide fixation, the same distribution was seen as in cells treated similarly but at room temperature (not shown).

## Non–pre-fixed Cells

In some experiments, cells were incubated with Con A–TNP for 5, 10, or 30 min at 37°C, before fixation. Fig. 12 shows the number of gold particles per $\mu m^2$, counted on dry-cleaved preparations. Numbers per $\mu m$ as counted on thin sections were converted to numbers per $\mu m^2$ assuming a section thickness of 90 nm. The latter data were in good agreement with those counted on dry-cleaved preparations. In both cases, the amount of label rapidly declined between 0 and 10 min after Con A–TNP application, and remained constant thereafter. At all times, the label remained dispersed as well as clustered, and an increase in clustering was not apparent.

## WGA on Hepatoma Cells and Con A on Hepatocytes

Results obtained with wheat germ agglutinin–TNP were quite similar to those described for Con A–TNP. Again, label was at the electron-dense membrane areas, dispersed as well as clustered. Label was virtually absent when the lectin was applied together with the hapten sugar N-acetylglucosamine. In preliminary experiments with isolated hepatocytes, the membrane-associated network was found to be denser than in the hepatoma cells. Nevertheless, all label was again localized in areas associated with the filaments, and absent from the small areas overlying openings in the network (not shown).
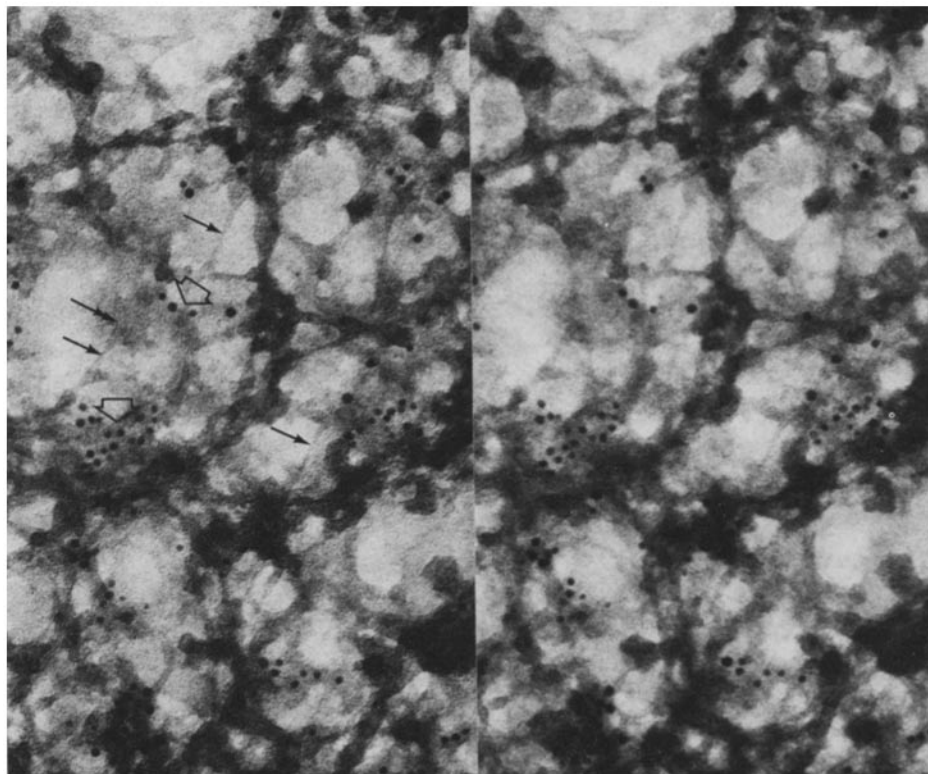


FIGURE 6   Enlargement of a part of Fig. 5. Note thin filaments (arrows) terminating at sites (double arrow) some distance to the cellular side of the gold label (open arrows). × 225,000.
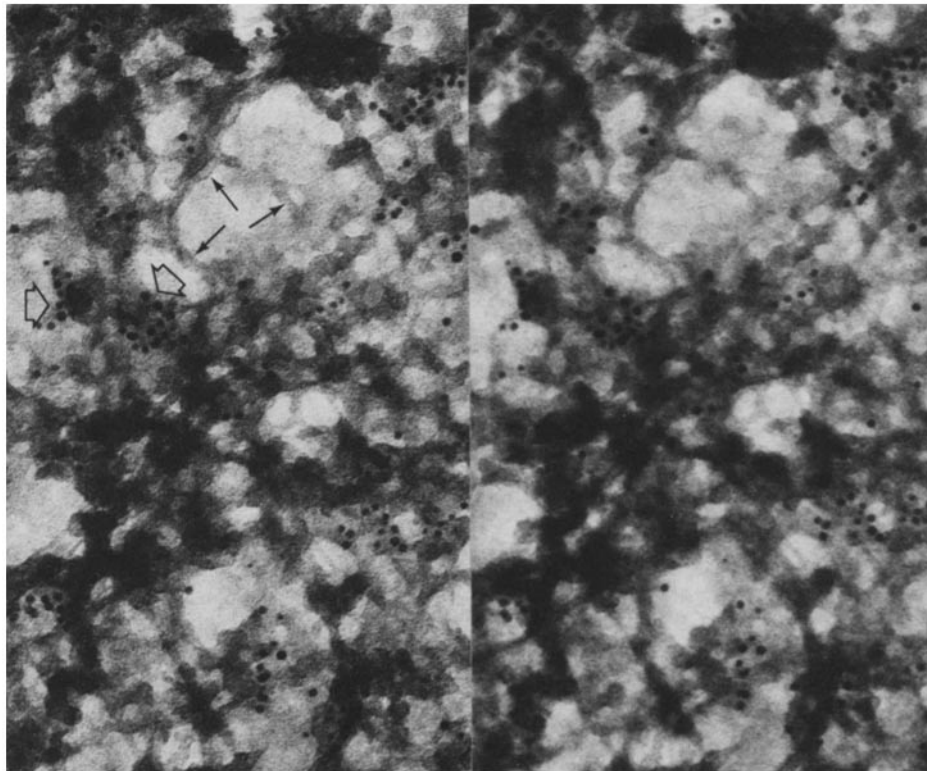
FIGURE 7   Enlargement of a part of the same preparation as in Fig. 5. Note strands of ~6 nm (arrows) and high electron density at the membrane where gold particles are clustered (open arrows). × 225,000.
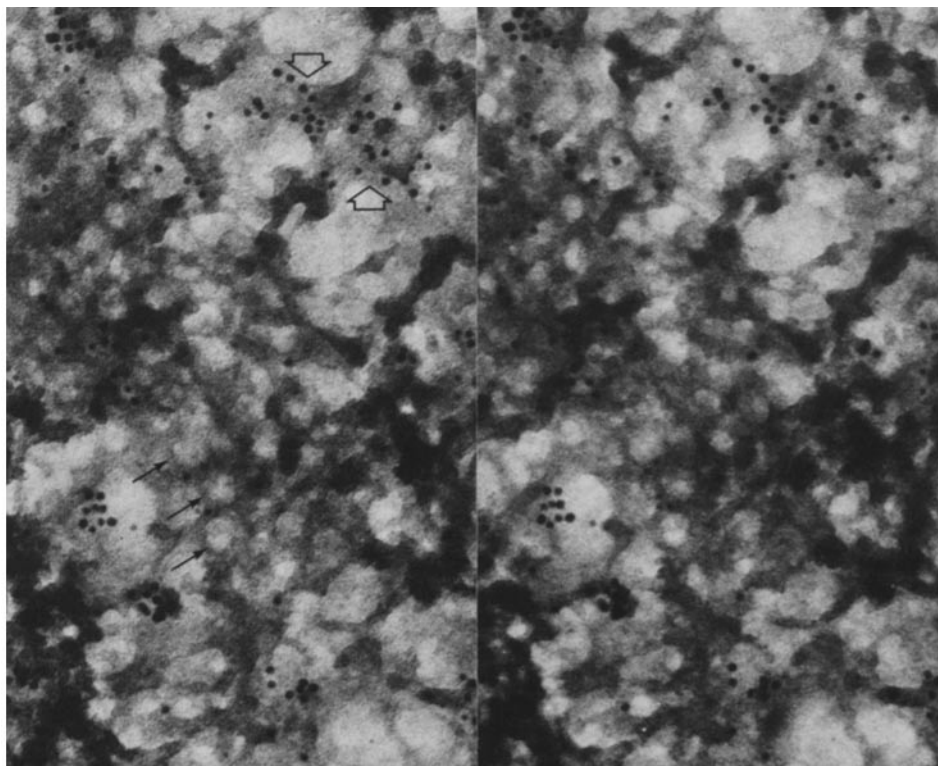


FIGURE 8   Enlargement of a part of Fig. 5. Note 6-nm strands in a hexagonal pattern (arrows), and labeled membrane (open arrows). × 225,000.
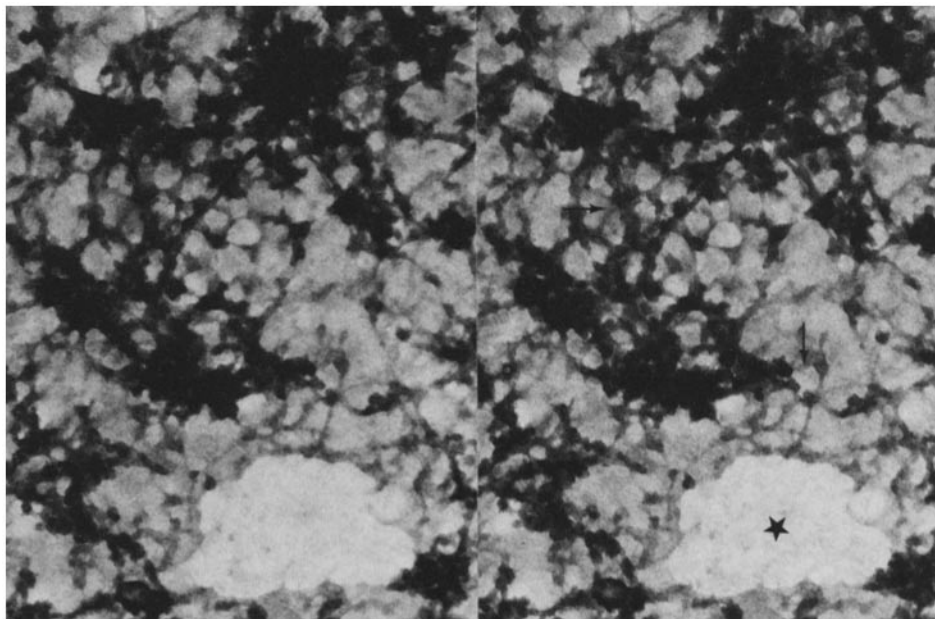
FIGURE 9   Dry-cleaved preparation of an unlabeled cell. Note electron-dense membrane areas (e.g., arrows). A hole can be seen in the membrane (star). × 112,500.
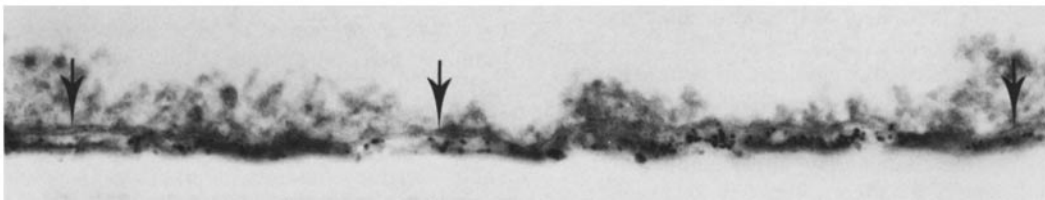


FIGURE 10   Dry-cleaved labeled cell embedded in Epon. The cell membrane remains intact (arrows) and the label remains located at the extracellular surface. × 112,500.
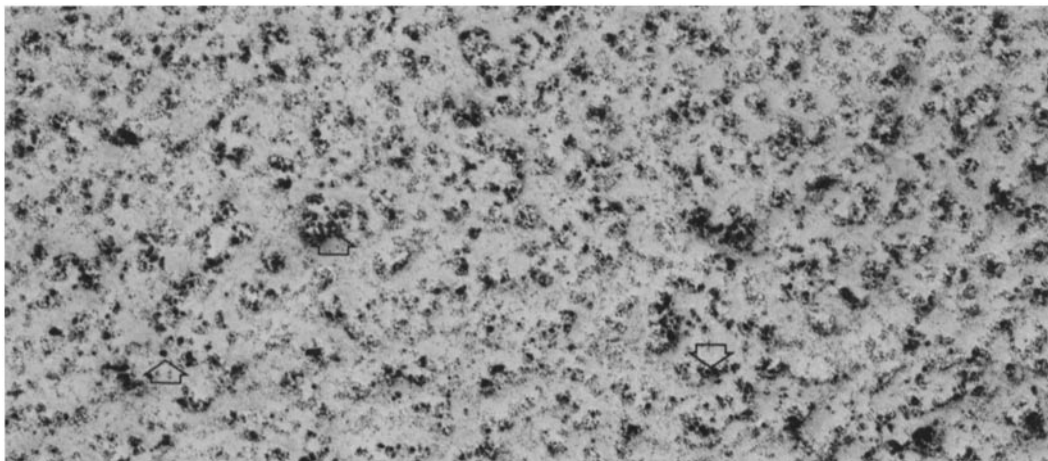


FIGURE 11   Replica of the upper surface of a critical point–dried H35 cell, which was not inverted and not cleaved. The black dots (see arrows for examples) are gold particles enclosed in the metal layer, which was kept very thin in order to facilitate visualization of the label. × 90,000.

## DISCUSSION

To visualize the topographical relation between membrane-associated filaments and membrane constituents, we combined immunogold labeling and dry-cleaving. To study the applicability of the method, we selected a particularly suitable model. The epithelial cell monolayers used had the advantage

that they could be easily detached and inverted, as was necessary to cleave the cells close to the medium-facing surface. Furthermore, we chose to visualize lectin-binding surface molecules, because they are numerous and because they can be labeled after fixation. However, preliminary results indicate that the method can also be applied to adherent fibroblasts as well as to suspended cells, and to the visualization of less
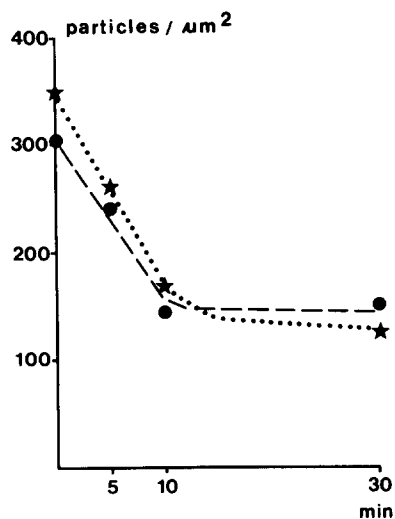
FIGURE 12 Number of gold particles counted on cells incubated with 500 μg/ml Con A–TNP at 37°C for various periods before fixation. ●, dry-cleaved preparations; ★, thin sections. In the latter case, numbers per μm² were calculated assuming a section thickness of 90 nm. Shown are the results of a representative experiment.

numerous molecules such as insulin receptors.

The presence of the gold label at the extracellular face of the membrane allowed us to localize that face in stereo micrographs. Many filaments appeared to terminate at a plane at some distance from the label. It seems likely that this plane was the intracellular face of the membrane. Different types of such filaments were observed, with an approximate thickness of either 2 or 6 nm, the latter sometimes arranged in a hexagonal pattern. The nature of the protein constituents of these filaments is not known. However, the dimensions of the hexagonal pattern suggested it to be composed of clathrin (42). Anyhow, it appears that membrane connections are not formed by a single type of filament.

The most striking result of this study was the observed distribution of lectin-binding surface constituents as revealed by our novel TNP–anti-TNP/protein A–gold labeling method. The label was not homogeneously distributed as might be expected based on observation of thin sections, but strikingly coincident with the pattern of the filament network. In stereo micrographs, virtually all label was seen to be localized to membrane areas of enhanced electron density, possibly equivalent to the "granular" patches seen at the erythrocyte membrane (43). This density may have been due to a comparatively high concentration of surface proteins at those areas. This observation suggested that protein-poor and protein-rich microdomains exist in the plasma membrane of the hepatoma cells as well as of hepatocytes. These microdomains were dispersed so finely that the divergence from homogeneous distribution was not observed in thin sections, and may therefore have gone undetected so far.

The possibility should be considered that the observed distribution was an artifact of our method. For instance, one might imagine that upon dry-cleaving, part of the label was selectively removed from certain membrane areas. This possibility seems remote because it would require the label to be pulled through the membrane and the cell cortex, which would evidently result in a perforated membrane. In damaged preparations, holes in the membrane can readily be seen (Fig. 9) and such holes were not observed at sites where label was

lacking. Furthermore, the amount of label was not different in dry-cleaved preparations compared to thin sections, assuming the latter to have a thickness of 90 nm, a reasonable assumption for sections with a light yellow interference color (44). Although admittedly section thickness cannot be exactly measured, this would seem to indicate that not a large part of the label is lost during the dry-cleaving procedure. Finally, in thin sections of embedded dry-cleaved preparations, the cell membrane was usually intact, and the location and distribution of the label not different from uncleaved cells (Fig. 10).

An alternative possibility is redistribution due to inadequate fixation. Cell surface proteins are not necessarily completely immobilized by glutaraldehyde fixation (45) and one might imagine that solitary, non-cross-linked proteins are still able to move after fixation until they collide with cytoskeleton-associated proteins, to which they might then be cross-linked. This movement should be severely restricted, if not annihilated, at 0°C (46, 47). However, when all treatments from glutaraldehyde fixation up to and including osmium tetroxide fixation were performed at 0°C, the same distribution of label was found, rendering this possibility less likely. Furthermore, free aldehyde groups were reacted with glycine and this should have prevented further cross-linking. A last possibility to be considered is redistribution of cell surface proteins induced, even after fixation, by attachment to the poly-L-lysine or by the dry-cleaving procedure. The observation that the distribution of label on replicas of the upper surface of cells that had not been inverted and not dry-cleaved (Fig. 11) was comparable to that in dry-cleaved cells, appears to exclude this possible artifact.

The concept of membrane microdomains has been postulated before, based on fluorescence polarization measurements of lipid fluidity (48). The present observations suggest a possible explanation for the existence of such membrane domains. If membrane proteins interact with membrane-associated filaments they would tend to be preferentially localized to sites where such filaments are present, even if the interactions are weak and transient. This would lead to protein-rich and protein-poor regions in the membrane. Differences in lipid fluidity might then be caused by interactions of lipids with proteins (49) or even by a different lipid composition of protein-rich areas, due to preferential association of proteins with particular lipids (50).

The localization of proteins to particular membrane areas is not necessarily in contrast to their observed mobility. The protein-rich areas were finely dispersed and interconnected so that proteins might readily diffuse through such areas albeit constrained by their interactions with the filaments. Their localization near membrane-associated filaments would allow instantaneous immobilization upon alteration of the affinity for those filaments after interaction with ligand (7–10).

The method described might be particularly useful to study alterations in membrane-associated filaments upon patching and capping of surface molecules. Con A–binding molecules on H35 hepatoma cells did not extensively redistribute after binding to Con A, so that this model is evidently not the most interesting in this respect. The only apparent change observed was a reduction in label within the first 10 min after exposure to Con A–TNP (Fig. 12). We have not extensively studied the reasons for this reduction. Internalization does not seem a likely explanation because, as previously described (38), these cells do not contain many coated vesicles. Alternatively, Con
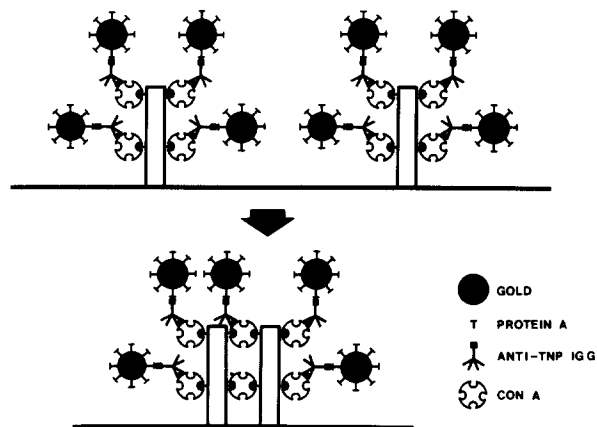
FIGURE 13 A proposed explanation for the reduction in particles as seen in Fig. 10. Due to limited cross-linking, determinants are bound by less Con A molecules, and some of these become unaccessible to gold particles.

A-TNP may have been shed from the cell. Our favored explanation is illustrated in Fig. 13. Upon limited cross-linking of proteins by Con A, part of the determinants may have become unaccessible to anti-TNP antibodies. In addition, several Con A-binding determinants, each able to bind a single lectin molecule on prefixed cells, are bound to the same lectin molecule after cross-linking, again leading to decreased over-all binding. Thus, one should realize that there is not necessarily a strict relation between the number of Con A-binding determinants present and the amount of label.

In summary, we have developed a method potentially useful for the study of membrane–cytoskeleton interactions in relation to cell surface protein mobility. Furthermore, we have observed an inhomogeneous distribution of surface glycoproteins and an apparent association of these proteins with membrane-associated filaments which, if found to be generally appicable, should be taken into account in models of membrane phenomena.

REFERENCES

1. Schlessinger, J., D. Axelrod, D. E. Koppel, W. W. Webb, and E. L. Elson. 1977. Lateral transport of a lipid probe and labeled proteins on a cell membrane. Science (Wash. DC). 195:307–309.
2. Schlessinger, J. 1979. Lateral diffusion of surface immunoglobulin, Thy-1 antigen, and a lipid probe in lymphocyte plasma membranes. Proc. Natl. Acad. Sci. USA. 76:5163–5167.
3. Jung, G., R. M. Helm, C. A. Carrothers Carraway, and K. L. Carraway. 1984. Mechanism of concanavalin A-induced anchorage of the major cell surface glycoproteins to the submembrane cytoskeleton in 13762 ascites mammary adenocarcinoma cells. J. Cell Biol. 98:179–187.
4. Koch, G. L. E., and M. J. Smith. 1978. An association between actin and the major histocompatibility antigen H-2. Nature (Lond.). 273:274–281.
5. Ben-Ze'ev, A., A. Duerr, F. Solomon, and S. Penman. 1979. The outer boundary of the cytoskeleton: a lamina derived from plasma membrane proteins. Cell. 17:859–865.
6. Mescher, M. F., M. J. L. Jose, and S. P. Balk. 1981. Actin-containing matrix associated with the plasma membrane of murine tumour and lymphoid cells. Nature (Lond.). 289:139–144.
7. Edelman, G. M. 1976. Surface modulation in cell recognition and cell growth. Science (Wash. DC). 192:218–226.
8. Henis, Y. I., and E. L. Elson. 1981. Inhibition of mouse lymphocyte surface immunoglobulins by locally bound Con A. Proc. Natl. Acad. Sci. USA. 78:1072–1076.
9. Woda, B. A., and M. L. McFadden. 1983. Ligand-induced association of rat lymphocyte membrane proteins with the detergent-insoluble lymphocyte cytoskeletal matrix. J. Immunol. 131:1917–1919.
10. Jesaitis, A. J., J. R. Naemura, L. A. Sklar, C. G. Cochrane, and R. G. Painter. 1984. Rapid modulation of N-formyl chemotactic peptide receptors on the surface of human

granulocytes: formation of high-affinity ligand-receptor complexes in transient association with cytoskeleton. J. Cell Biol. 98:1378–1387.
11. Geiger, B. 1983. Membrane-cytoskeleton interaction. Biochim. Biophys. Acta. 737:305–341.
12. Sundqvist, K. G., and A. Ehrnst. 1976. Cytoskeletal control of surface membrane fluidity. Nature (Lond.). 264:226–231.
13. Bourguignon, L. Y. W., and S. J. Singer. 1977. Transmembrane interactions and the mechanisms of capping of surface receptors by their specific ligands. Proc. Natl. Acad. Sci. USA. 74:5031–5035.
14. Bourguignon, L. Y. W., M. L. Nagpal, K. Balazovich, V. Guerriero, and A. R. Means. 1982. Association of myosin light chain kinase with lymphocyte membrane-cytoskeleton complex. J. Cell Biol. 95:793–797.
15. Levine, J., and M. Willard. 1983. Redistribution of fodrin (a component of the cortical cytoplasm) accompanying capping of cell surface molecules. Proc. Natl. Acad. Sci. USA. 80:191–195.
16. Nelson, W. J., C. A. L. S. Colaco, and E. Lazarides. 1983. Involvement of spectrin in cell-surface receptor capping in lymphocytes. Proc. Natl. Acad. Sci. USA. 80:1626–1630.
17. Hirokawa, N., and L. G. Tilney. 1982. Interactions between actin filaments and membranes in quick-frozen and deeply etched hair cells of the chick ear. J. Cell Biol. 95:249–261.
18. Avnur, Z., J. V. Small, and B. Geiger. 1983. Actin-independent association of vinculin with the cytoplasmic aspect of the plasma membrane in cell-contact areas. J. Cell Biol. 96:1622–1630.
19. Howe, C. L., and M. S. Mooseker. 1983. Characterization of the 110-kdalton actin-, calmodulin-, and membrane-binding protein from microvilli of intestinal epithelial cells. J. Cell Biol. 97:974–985.
20. Petrini, M., D. L. Emerson, and R. M. Galbraith. 1983. Linkage between surface immunoglobulin and cytoskeleton of B-lymphocytes may involve Gc protein. Nature (Lond.). 306:73–74.
21. Burridge, K., and P. Mangeat. 1984. An interaction between vinculin and talin. Nature (Lond.). 308:744–745.
22. Brown, S. S., H. L. Malinoff, and M. S. Wicha. 1983. Connectin: cell surface protein that binds both laminin and actin. Proc. Natl. Acad. Sci. USA. 80:5927–5930.
23. D'Angelo Siciliano, J., and S. W. Graig. 1982. Meta-vinculin, a vinculin-related protein with solubility properties of a membrane protein. Nature (Lond.). 300:533–535.
24. Tarone, G., R. Ferracini, G. Galetto, and P. Comoglio. 1984. A cell surface integral membrane glycoprotein of 85,000 mol wt (gp85) associated with Triton-X-100-insoluble cell skeleton. J. Cell Biol. 99:512–519.
25. Glenney, J. R., and P. Glenny. 1984. The microvillus 110K cytoskeletal protein is an integral membrane protein. Cell. 37:743–751.
26. Mangeat, P., and K. Burridge. 1984. Actin-membrane interaction in fibroblasts: what proteins are involved in this assocition? J. Cell Biol. 99(1, Pt. 2):95s–103s.
27. Cherry, R. J. 1979. Rotational and lateral diffusion of membrane proteins. Biochim. Biophys. Acta. 559:289–327.
28. Vaz, W. L., K. Jacobson, E. S. Wu, and Z. Derzko. 1979. Lateral mobility of an amphiphatic apolipoprotein, ApoC-III, bound to phosphatidylcholine bilayers with and without cholesterol. Proc. Natl. Acad. Sci. USA. 76:5645–5649.
29. Branton, D., C. M. Cohen, and J. Tyler. 1981. Interaction of cytoskeletal proteins on the human erythrocyte membrane. Cell. 24:24–32.
30. Gratzer, W. B. 1981. The red cell membrane and its cytoskeleton. Biochem. J. 198:1–8.
31. Sheetz, M. P., M. Schindler, and D. E. Koppel. 1980. Lateral mobility of integral membrane proteins is increased in spherocytic erythrocytes. Nature (Lond.). 285:510–512.
32. Levine, J., and M. Willard. 1981. Fodrin: axonally transported polypeptides associated with the internal periphery of many cells. J. Cell Biol. 90:631–643.
33. Repasky, E. A., B. L. Granger, and E. Lazarides. 1982. Widespread occurrence of avian spectrin in non-erythroid cells. Cell. 29:821–833.
34. Glenney, J. R., and P. Glenney. 1983. Fodrin is the general spectrin-like protein found in most cells whereas spectrin and the TW protein have a restricted distribution. Cell. 34:503–512.
35. Mangeat, P. H., and K. Burridge. 1984. Immunoprecipitation of non-erythrocyte spectrin within live cells following micro-injection of specific antibodies: relation to cytoskeletal structures. J. Cell Biol. 98:1363–1377.
36. Tank, D. W., E. S. Wu, and W. W. Webb. 1982. Enhanced molecular diffusibility in muscle membrane blebs: release of lateral constraints. J. Cell Biol. 92:207–212.
37. Mesland, D. A. M., H. Spiele, and E. Roos. 1981. Membrane-associated cytoskeleton and coated vesicles in cultured hepatocytes visualized by dry-cleaving. Exp. Cell Res. 132:169–184.
38. Mesland, D. A. M., and H. Spiele. 1983. Plasma membrane-associated filament systems in cultured cells visualized by dry-cleaving. J. Cell Sci. 64:351–364.
39. Mesland, D. A. M., and H. Spiele. 1984. Brief extraction with detergent induces the appearance of many plasma membrane-associated microtubules in hepatocytic cells. J. Cell Sci. 68:113–137.
40. Okuyama, T., and K. Satake. 1960. On the preparation of 2,4,6-trinitrophenylamino acids and -peptides. J. Biochem. 47:454–466.
41. Slot, J. W., and H. J. Geuze. 1981. Sizing of protein A-colloidal gold probes for immunoelectron microscopy. J. Cell Biol. 90:533–536.
42. Heuser, J. 1980. Three dimensional visualization of coated vesicle formation in fibroblasts. J. Cell Biol. 84:560–583.
43. Tsukita, S., S. Tsukita, and H. Ishikawa. 1980. Cytoskeletal network underlying the human erythrocyte membrane. J. Cell Biol. 85:567–576.
44. Reid, N. 1975. Ultramicrotomy. Practical Methods in Electron Microscopy. Volume 3.II. A. M. Glauert, editor. North Holland/Elsevier, Amsterdam.
45. Jost, P., U. J. Brooks, and O. H. Griffith. 1973. Fluidity of phospholipid bilayers and membranes after exposure to osmium tetroxide and glutaraldehyde. J. Mol. Biol. 76:313–318.
46. Wu, E. A., K. Jacobson, and D. Papahadjopoulos. 1977. Lateral diffusion in phospholipid bilayers measured by fluorescence recovery after photobleaching. Biochem. J. 16:3936–3941.
47. Smith, B. A., and H. M. McConnell. 1978. Determination of molecular motion in membranes using periodic pattern photobleaching. Proc. Natl. Acad. Sci. USA. 75:2759–2763.
48. Karnovsky, M. J., A. M. Kleinfeld, R. L. Hoover, and R. D. Klausner. 1982. The concept of lipid domains in membranes. J. Cell Biol. 94:1–6.
49. Jain, M. K., and H. B. White. 1978. Long-range order in biomembranes. Adv. Lipid Res. 15:1–60.
50. Van Zoelen, E. J. J., R. F. A. Zwaal, F. A. M. Reuvers, R. A. Demel, and L. L. M. Van Deenen. 1977. Evidence for the preferential interaction of glycophorin with negatively charged phospholipids. Biochim. Biophys. Acta. 464:482–492.